NASA/TM–20210015330

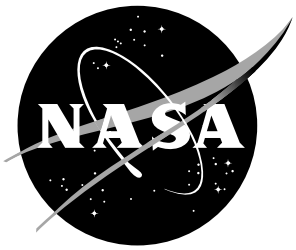

# Mars Exploration Rovers EDL Trajectory and Atmosphere Reconstruction Using NewSTEP

*Rohan G. Deshmukh and Christopher D. Karlgaard*
*Analytical Mechanics Associates, Hampton, Virginia*

May 2021

# NASA STI Program Report Series

Since its founding, NASA has been dedicated to the advancement of aeronautics and space science. The NASA scientific and technical information (STI) program plays a key part in helping NASA maintain this important role.

The NASA STI program operates under the auspices of the Agency Chief Information Officer. It collects, organizes, provides for archiving, and disseminates NASA's STI. The NASA STI program provides access to the NTRS Registered and its public interface, the NASA Technical Reports Server, thus providing one of the largest collections of aeronautical and space science STI in the world. Results are published in both non-NASA channels and by NASA in the NASA STI Report Series, which includes the following report types:

- TECHNICAL PUBLICATION. Reports of completed research or a major significant phase of research that present the results of NASA Programs and include extensive data or theoretical analysis. Includes compilations of significant scientific and technical data and information deemed to be of continuing reference value. NASA counterpart of peer-reviewed formal professional papers but has less stringent limitations on manuscript length and extent of graphic presentations.

- TECHNICAL MEMORANDUM. Scientific and technical findings that are preliminary or of specialized interest, e.g., quick release reports, working papers, and bibliographies that contain minimal annotation. Does not contain extensive analysis.

- CONTRACTOR REPORT. Scientific and technical findings by NASA-sponsored contractors and grantees.

- CONFERENCE PUBLICATION. Collected papers from scientific and technical conferences, symposia, seminars, or other meetings sponsored or co-sponsored by NASA.

- SPECIAL PUBLICATION. Scientific, technical, or historical information from NASA programs, projects, and missions, often concerned with subjects having substantial public interest.

- TECHNICAL TRANSLATION. English-language translations of foreign scientific and technical material pertinent to NASA's mission.

Specialized services also include organizing and publishing research results, distributing specialized research announcements and feeds, providing information desk and personal search support, and enabling data exchange services.

For more information about the NASA STI program, see the following:

- Access the NASA STI program home page at http://www.sti.nasa.gov

- Help desk contact information:

https://www.sti.nasa.gov/sti-contact-form/
and select the "General" help request type.

NASA/TM–20210015330

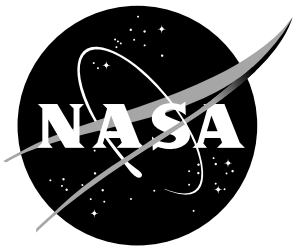

# Mars Exploration Rovers EDL Trajectory and Atmosphere Reconstruction Using NewSTEP

*Rohan G. Deshmukh and Christopher D. Karlgaard*
*Analytical Mechanics Associates, Hampton, Virginia*

National Aeronautics and
Space Administration

Langley Research Center
Hampton, Virginia 23681-2199

May 2021

## Acknowledgments

The content of this work benefited from discussions with Soumyo Dutta and Mark Schoenenberger (NASA Langley).



Available from:

NASA STI Program / Mail Stop 148
NASA Langley Research Center
Hampton, VA 23681-2199
Fax: 757-864-6500

## Abstract

This document describes the trajectory and atmosphere reconstruction of the Mars Exploration Rovers (Spirit and Opportunity) Entry, Descent, and Landing using the New Statistical Trajectory Estimation Program. The approach utilizes a Kalman filter to blend inertial measurement unit data with initial conditions and radar altimetry to obtain the inertial trajectory of the entry vehicle. The nominal aerodynamic database is then used in combination with the sensed accelerations to obtain estimates of the atmosphere-relative state. The reconstructed atmosphere profile is then blended with pre-flight models to construct an estimate of the as-flown atmosphere.


## 1 Introduction

On January 4th and January 25th, 2004, the Spirit and Opportunity rovers successfully conducted their respective Entry, Descent, and Landing (EDL) sequences to land on the surface of Mars. Data from the on-board Inertial Measurement Unit (IMU) (accelerations and angular rates) and Orbit Determination (OD)-derived initial conditions were utilized to reconstruct the as-flown trajectory of the entry vehicle from entry interface to parachute deployment using a dead reckoning integration technique. The nominal vehicle aerodynamic database was used to estimate the as-flown atmospheric density profile by solving for the density using the measured axial acceleration and the nominal axial force coefficient.

The methodology and results of the trajectory and atmospheric reconstruction are documented in [1]. Unfortunately, the reconstructed data has subsequently been lost. However, the raw telemetry data from the mission still exists and so can be used to reconstruct the trajectory and atmosphere for archival purposes. Unlike existing MER reconstructions, the reconstruction outlined in the paper makes use of the New Statistical Trajectory Estimation Program (NewSTEP). NewSTEP is an Iterative Extended Kalman Filter (IEKF) [10] code for processing various types of on-board and ground-based (where applicable) measurements to produce a trajectory estimate that is a best fit to all of the data sources based on their given uncertainties. It has been extensively utilized in post-flight trajectory reconstruction both at Earth [13, 14, 16] and at Mars [5, 15, 17].

This memorandum serves to document this reconstruction and the results. The remainder of the document is organized as follows. The next section provides a brief overview of the Mars Exploration rover entry vehicles and the nominal EDL timeline, and then gives an overview of the various measurement data sources that are used for the trajectory reconstruction. The following section provides an overview of the trajectory and atmosphere reconstruction methodology, before presenting the results of the reconstruction.

## 2 Vehicle Description

The Mars Exploration Rover (MER) mission consisted of twin rovers named Spirit and Opportunity. Both rovers were launched on two separate launches and entered the atmosphere of Mars on two separate trajectories. Both rovers utilized the same entry vehicle design consisting of a 70° sphere cone shape with a diameter of 2.65 m and mass at entry of 840 kg. The EDL concept of operations utilized by both rovers, as shown in Figure 1, is nearly identical to the previous Mars Pathfinder mission. Prior to entering the atmosphere ballistically, each entry vehicle is spin stabilized at 2 rpm with no active guidance or control system. Upon entering the atmosphere, the vehicles rely on passive aerodynamic stability for performing controlled descent. After reaching a dynamic pressure of 700 N/m$^2$, the supersonic disk-gap-band parachutes are deployed [3]. Shortly thereafter the heatshield is jettisoned, bridle is deployed, and the radar altimeter is activated to commence powered flight. Prior to retrorocket ignition, airbag landing system is inflated. The retrockets are utilized in the terminal descent phase on a gravity turn trajectory until the ground-relative vertical velocity is nullified at a height of 12m above the surface. At this point, the bridle is cut and the airbag system housing the rovers freefalls to the surface. The system absorbs the impact energy upon consecutive bounces on the surface until the system reaches a rest. Additional details on the vehicle design and EDL system overview can be found in [3].

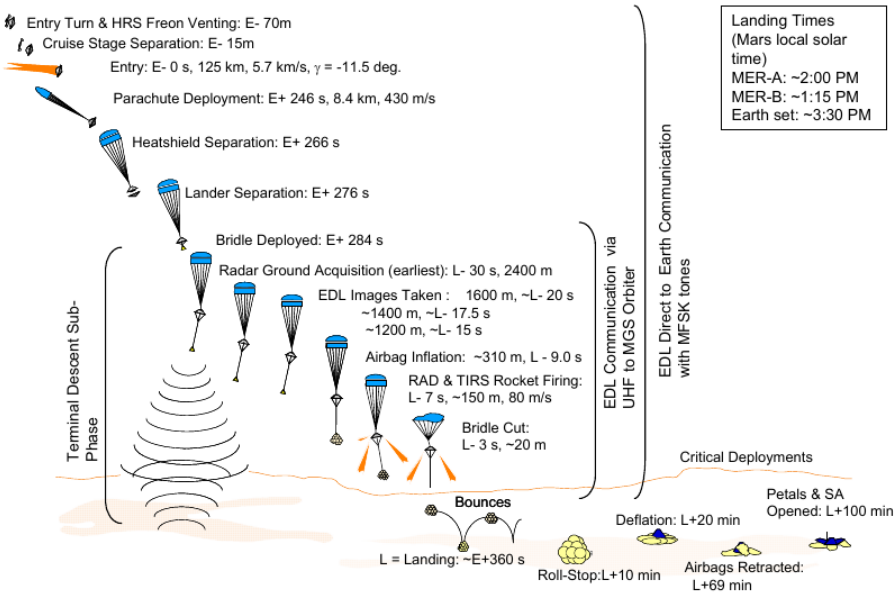


Figure 1: Mars Entry Rovers Entry, Descent, and Landing. Imaged adapted from [3]

Coordinate frames relevant to the vehicle aerodynamics and flight mechanics are shown in Figure 2. The axes labeled $X_C$, $Y_C$, and $Z_C$ are the axes of the cruise frame and the axes labeled $X_B$, $Y_B$, and $Z_B$ define the flight mechanics body frame. The cruise frame is an estimate for the orientation of the transformed IMU data. More information on the IMU can be found in the next section. Directions of the

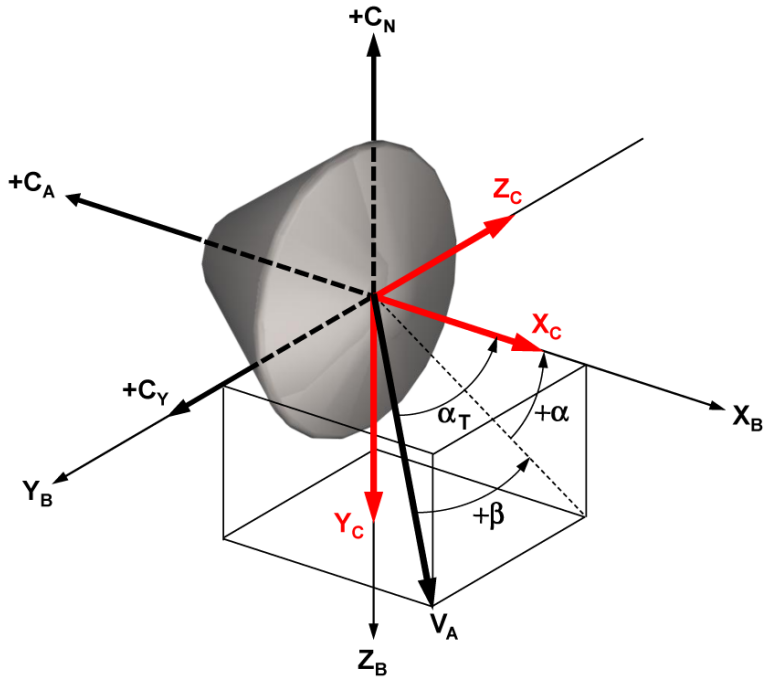


Figure 2: MER Coordinate Frames. Image adapted from [5]

aerodynamic force coefficients $C_A$ (axial), $C_Y$ (side), and $C_N$ (normal) are shown relative to the flight mechanics body frame as are the definitions of the aerodynamic flow angles. These angles consist of the total angle of attack, $\alpha_t$, angle of attack, $\alpha$, and side-slip angle, $\beta$. The transformation from cruise frame to the flight mechanics body frame is given by

$$T_{cr2b} = \begin{bmatrix} 1 & 0 & 0 \\ 0 & 0 & -1 \\ 0 & 1 & 0 \end{bmatrix} \tag{1}$$

## 3 Data Sources

At the time of this writeup, the available MER flight data are limited to IMU data and radar altimeter data. The nominal vehicle states at atmospheric entry, parachute deployment, and surface impact come from literature. For Spirit, the full IMU data along with radar data are available. For Opportunity, only the IMU data up until parachute deployment are available. The altimeter and altimetry rate data data sources come from measurements at low altitudes ($\leq$ 2500 m) during the parachute descent phase [1]. Both these data sources are utilized to validate the reconstructed trajectory. Furthermore, post landing radio measurements can be utilized to ascertain the landing site, if available. The following subsections describe these data sources.

### 3.1 Inertial Measurement Unit

The primary measurement source for performing the trajectory and atmosphere reconstruction is the on-board IMU, which provides three axis linear acceleration and angular rate measurements in the IMU instrument frame. The IMU instrument suite consisted of two Litton LN-200s containing fiber optic gyros for rotational measurements and silicon accelerometers for acceleration measurements. The IMUs were located in the rover and backshell of each vehicle. Figure 3 provides a visualization of each MER entry vehicle, whose forebody consists of a sphere-cone heatshield and aftbody consists of the backshell. Each rover is housed inside the vehicle. The exact location and orientation relative to the vehicle body-frame is unknown for the rover and backshell IMUs. The IMUs produced data at a rate of 400 Hz. The onboard flight computer on each vehicle downsampled this fast data rate down to 8Hz via averaging of 50 sec intervals. The acceleration and rotational measurements are provided at 8 Hz. More detailed information on the IMU instrumentation can be found in [8]. The spacecraft clock time (SCLK) provided in IMU data is biased based off a reference time, which is equal to 126460000 sec and 128270000 sec for Spirit and Opportunity respectively. In the subsequent figures below, the plotted time series is adjusted such that atmospheric entry interface occurs at zero time. The corresponding SCLK for atmospheric entry is 2085.625 sec for Spirit and 8194.625 sec for Opportunity [2].

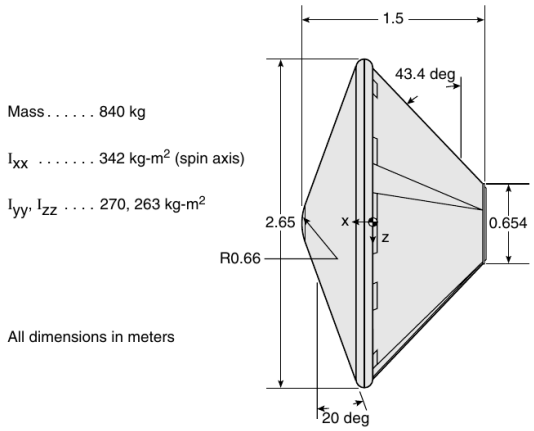


Figure 3: MER Entry Vehicle Configuration

In addition to downsampling the raw IMU data, the onboard flight computer on each vehicle computed an additional transformed dataset. This dataset transforms the raw IMU measurements at 8 Hz to each vehicle's center of mass. The rotational data for both the rover and backshell are reported in quaternions. In the available transformed IMU datasets, only the backshell data are reported. For Spirit the data time series available goes from entry interface to landing whereas for Opportunity the data time series available goes from entry interface up until parachute deployment. For the sake of consistency, only the transformed backshell IMU data are analyzed further in this report. The transformed IMU acceleration measurements for Opportunity are shown in Figure 4 and for Spirit are shown in Figure 5.

The quaternion data are defined relative to EMEJ2000 reference frame [12]. The quaternions are transformed to the inertial frame utilizing a methodology outlined in [1]. Blanchard does note that the sun line angle used in the methodology is unknown and can be varied until EDL metrics is minimized (e.g. landing site error). In this report, a similar constant sun line angle of -0.75 deg is assumed. Assuming a 3-2-1 Euler Angle scheme, the body-to-inertial Euler rotational angles and rates are computed using the transformed quaternions. Despite the quaternions already providing knowledge of the rotational evolution of each vehicle, the rotational rate data are still utilized by the trajectory reconstruction algorithm and can be used as a sanity check to the expected rotation of each vehicle. The rotational rate and acceleration data, plotted from atmospheric interface, is shown in Figure 4 and Figure 5. Upon entering the atmosphere, the resulting roll rate for both vehicles is near 12 °/s, or approx. 2 RPM, which is consistent with the exoatmospheric spin stabilization rate.

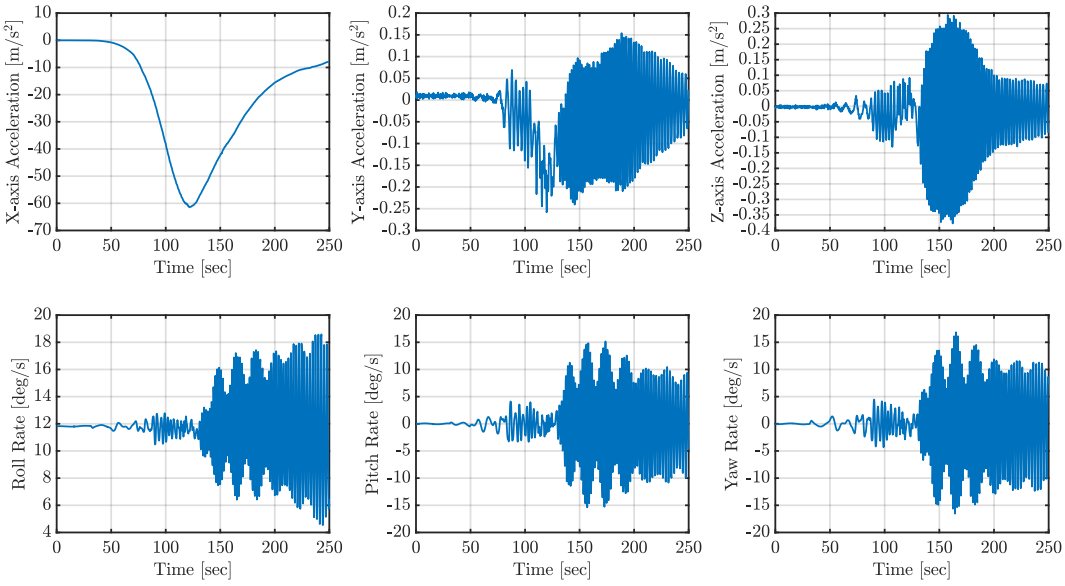


Figure 4: MER-1 (Opportunity) Backshell Accelerations and Angular Rates transformed to vehicle center of mass. Results are reported in flight mechanics body frame.

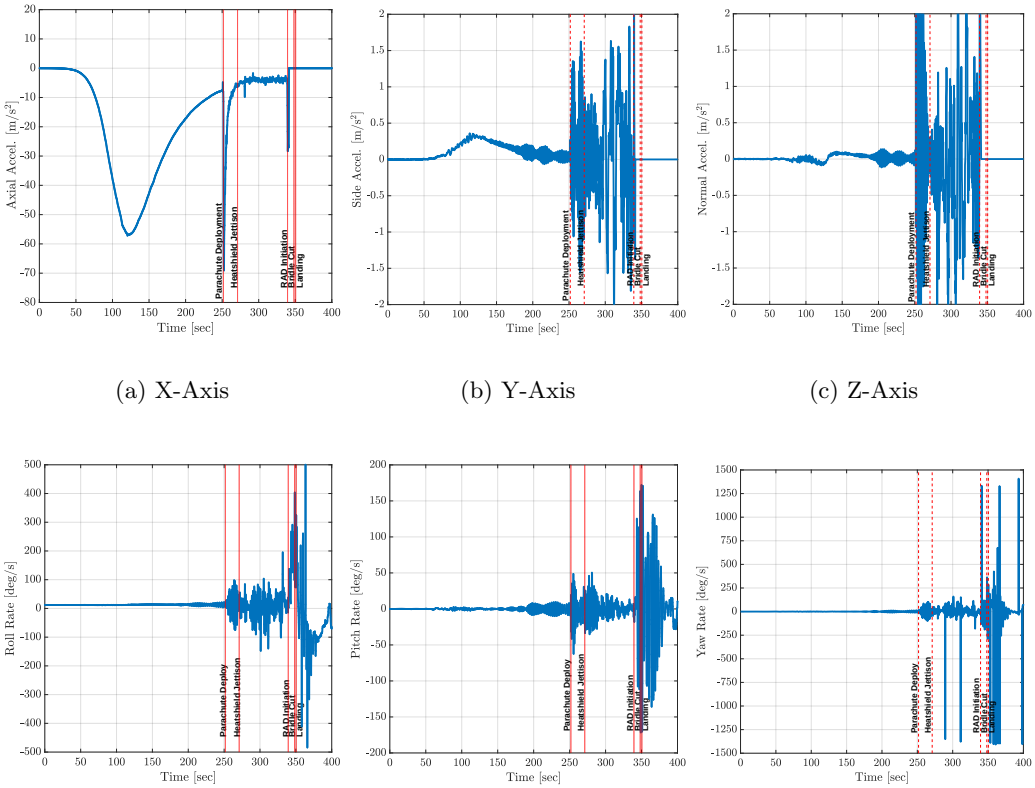


(a) X-Axis (b) Y-Axis (c) Z-Axis

(d) X-Axis (e) Y-Axis (f) Z-Axis

Figure 5: MER-2 (Spirit) Backshell Accelerations and Angular Rates transformed to vehicle center of mass. Results are reported in flight mechanics body frame.

### 3.2 Initial Conditions

The initial conditions used for the reconstruction are based on the orbit determination (OD) solution OD77 [11]. The states are provided in the Earth Mean Equator of January 2000 (EMEJ2000) [12] inertial frame at atmospheric entry. These coordinates correspond to a radius from the center of the planet of 3522.2 km for Spirit and Opportunity. The cartesian position and velocity components are listed in Table 1. The OD uncertainties are not included in this report.

The initial attitude of each vehicle is assumed from the transformed quaternion dataset. The attitude conditions at entry interface, $t_0$, are listed in Table 2.

Transforming these set of quaterions to the inertial frame yields the following initial conditions as shown in Table 3. Note that these values can potentially vary depending on the assumptions made in the transformation.

Table 1: EMEJ2000 Orbit Determination 77 Initial Conditions

| Coordinate | Initial Condition (Spirit) | Initial Condition (Opportunity) |
|---|---|---|
| $X$, m | -2832174.6582 | -3126180.414 |
| $Y$, m | -1797708.0539 | -1612747.6238 |
| $Z$, m | -1073743.5906 | -178700.7583 |
| $\dot{X}$, m/s | 3532.8316 | 3546.2262 |
| $\dot{Y}$, m/s | -4169.9156 | -4443.0415 |
| $\dot{Z}$, m/s | 1341.776 | 397.6862 |

Table 2: EMEJ2000 Cruise Frame Attitude Initial Conditions

| Quaternion | Initial Condition (Spirit) | Initial Condition (Opportunity) |
|---|---|---|
| $e_0$ | -0.742139 | -0.082974 |
| $e_1$ | 0.272225 | 0.834244 |
| $e_2$ | -0.582497 | -0.036695 |
| $e_3$ | 0.189263 | 0.543880 |

Table 3: EMEJ2000 Inertial Frame Attitude Initial Conditions

| Quaternion | Initial Condition (Spirit) | Initial Condition (Opportunity) |
|---|---|---|
| $e_0$ | 0.057208 | 0.707708 |
| $e_1$ | -0.767490 | -0.153508 |
| $e_2$ | -0.633233 | -0.289977 |
| $e_3$ | -0.081868 | 0.625698 |

### 3.3 Aerodynamics Model

The aerodynamics model is only utilized in the atmospheric reconstruction phase. Due to not having the MER aerodynamic databases [6] at the time of this writeup, the Mars Phoenix aerodynamic database is used as a placeholder. The MER and Phoenix aeroshell geometries are nearly identical with similar heatshield diameters, nose radii, and sphere-cone angles [9]. The aerodynamics model for the Phoenix entry vehicle was developed using a combination of historical data, previous flight tests of similar systems, wind tunnel testing, and computational methods. The Phoenix entry vehicle was geometrically similar to the Mars Exploration Rover, Pathfinder, and Viking geometries and leveraged this data as appropriate. This approach allowed an aerodynamic database to be generated that encompassed all of the flight regimes, including free molecular, transitional, hypersonic, supersonic, and transonic flows. The resultant database included static and dynamic coefficients with

associated uncertainties (note: these uncertainties are not utilized in this report). The final aerodynamic database product is a model that can be queried flight conditions and return the relevant aerodynamic coefficients for trajectory simulations. A detailed description and analysis of the Phoenix aerodynamic database can be found in [20].

### 3.4 Gravity Model

The Mars gravitational acceleration is modeled using the MRO110C model [21]. This model is based on tracking data of Mars Global Surveyor (MGS), Mars Odyssey and Mars Reconnaissance Orbiter (MRO), and MOLA-derived topography data. The model contains spherical harmonics up to degree and order 110.

## 4 Reconstruction Methods

The reconstruction process utilized for the MER EDL data consists of three steps as shown in Figure 6. In the first step, the IMU datasets are processed to be compatible with NewSTEP code. This process was explained in the previous section with results shown by Figure 4 and Figure 5. In the second step, the NewSTEP code is used to generate a kinematic reconstruction of the inertial flight path of the vehicle based off orbit determination initial conditions, IMU data, parachute deployment state, and landing site coordinates. In the third step, the reconstructed trajectory along with the vehicle aerodynamic database are both utilized to reconstruct the atmospheric profile of the flown trajectory. *The reconstruction produced in this paper is deterministic as no uncertainty is modeled.*


Figure 6: MER Reconstruction Process

Through trial-and-error, it was found that solely integrating the transformed IMU rotational rate data for either vehicle produced inconsistent reconstructed trajectories. These trajectories required unrealistic modifications to the initial states in order to produce feasible trajectories. Such an example included modification on the entry flight path angle by a few degrees, despite this value being generally known (see Figure 1), such that the reconstructed trajectory reached the vicinity of the parachute deployment state. If this modification is not done, then the subsequent reconstructed trajectory impacts the surface prematurely. Other challenges faced with utilizing the rotational rate data included reconstructing the trajectory after parachute deployment. As shown in Figure 5, the rapid oscillations in rotational rate data after parachute deployment led to challenges in the accuracy of the reconstructed trajectory as compared to the available altimeter data.

As a result, an assumption is made to the flight condition to eliminate the dependence of rotational rate data. Each vehicle is assumed to fly at zero total angle of attack. This assumption was utilized by Blanchard et al. [1] and is generally a good approximation for ballistic flight. The NewSTEP code is modified to achieve this flight condition.

In the next step, the nominal aerodynamic database and sensed accelerations are used to reconstruct the atmospheric-relative trajectory. Dynamic pressure is computed from the axial acceleration, mass, and reference area. The flow angles are simultaneously computed from the ratio of lateral to axial acceleration. The density is computed from the dynamic pressure and the reconstructed velocity (assuming the nominal winds), and then static pressure is computed from an integration of the hydrostatic equation. An estimate of the Mach number can be computed from the static and dynamic pressure. Again, a deterministic process is assumed. The overall process is described in [18, 19].

# 5 Reconstruction Results

The results of the reconstruction process described in the previous section are shown in the following subsections, describing the inertial trajectory, atmospheric-relative trajectory, and the atmosphere reconstruction.

## 5.1 Inertial Trajectory

Figure 7 and Figure 8 provide a comparison between the altitude and relative-velocity time histories of the present reconstruction and one produced in Reference [1] for Opportunity and Spirit, respectively. Up until the parachute deployment, the altitude and velocity profiles for both vehicles nearly match. For Spirit, the present reconstruction agrees well with Reference [1] after parachute deployment up until the retrorocket initiation. Figure 8 shows an increase in the relative velocity after the initiation. More details on this anomaly are explained in the subsequent paragraph.

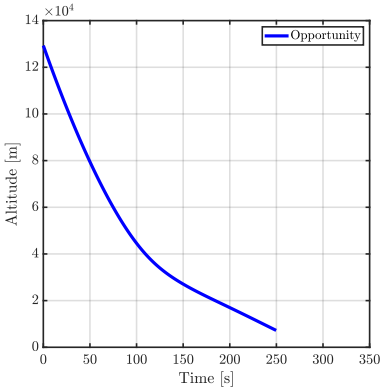


(a) Reconstruction

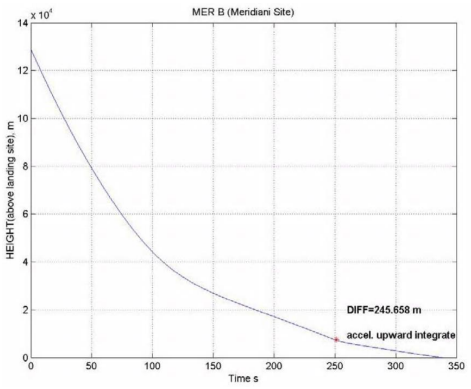


(b) Reference [1]

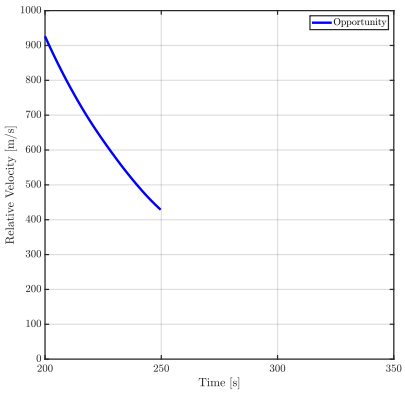


(c) Reconstruction

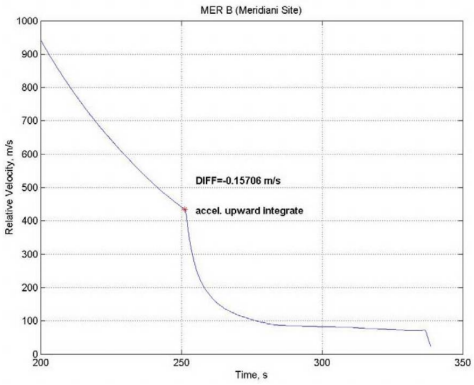


(d) Reference [1]

Figure 7: Comparison of Areodetic Altitude and Relative Velocity for Opportunity/MER-B

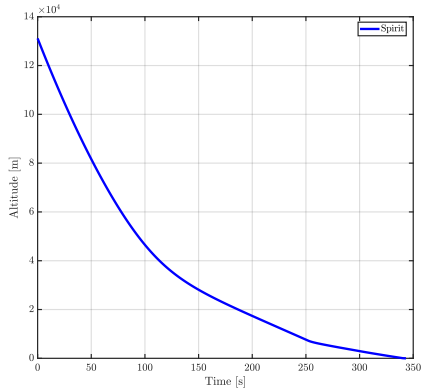


(a) Reconstruction

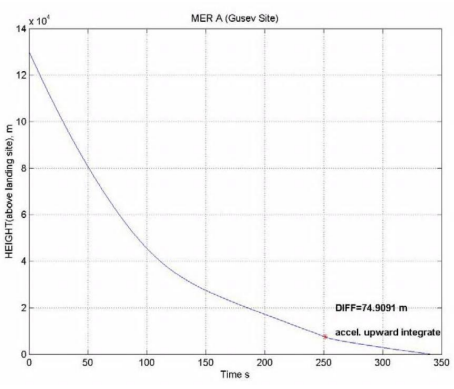


(b) Reference [1]

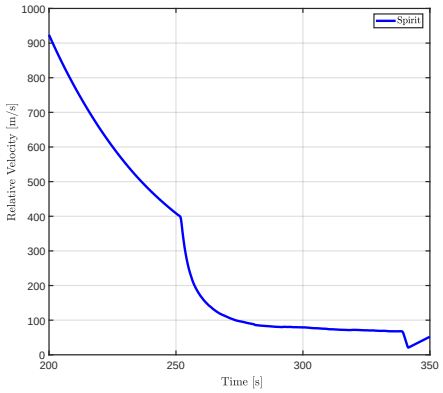


(c) Reconstruction

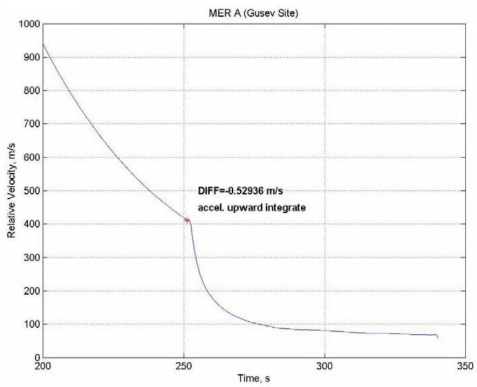


(d) Reference [1]

Figure 8: Comparison of Areodetic Altitude and Relative Velocity for Spirit/MER-A

Figure 9 provides the reconstructed position and velocity time histories of both vehicles from atmospheric entry to parachute deployment (Opportunity) or landing (Spirit). For comparison to existing reconstructions in the literature, data tips are added in Figure 9 at parachute deployment for both vehicles. The current reconstruction shows Spirit and Opportunity to have flow similar altitude profiles as well as similar latitude/longitude profiles despite having different initial conditions. Furthermore, the current reconstruction shows similar profiles for the north-east-down velocity components between Spirit and Opportunity despite the differences in initial conditions. Due to the higher latitude of Spirit's trajectory at entry, the initial north velocity component is much larger than Opportunity's.

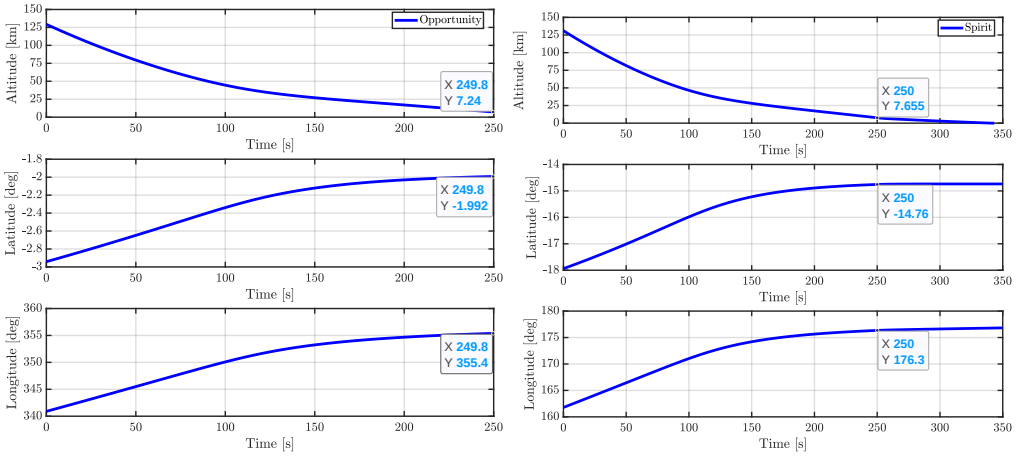


(a) Position (Opportunity)




(b) Position (Spirit)

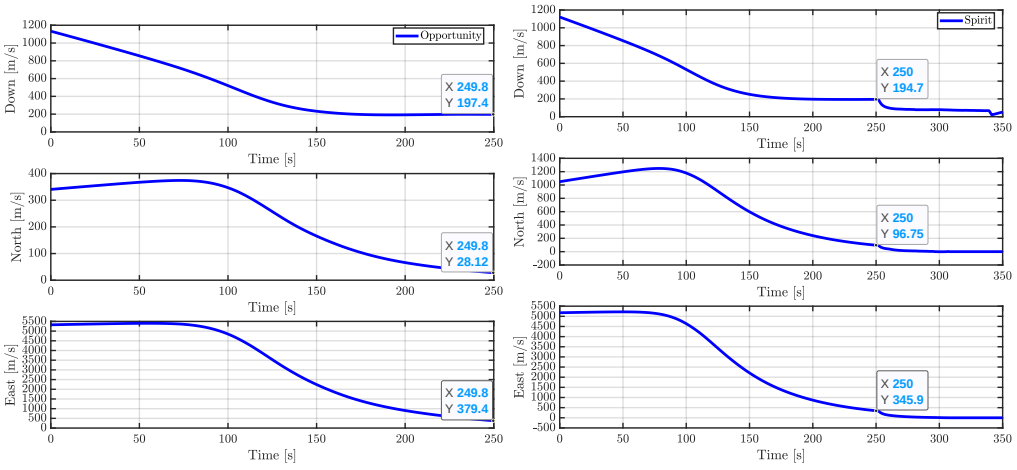


(c) Velocity (Opportunity)




(d) Velocity (Spirit)

Figure 9: Trajectory Reconstructions for MER Rovers. Data tips located at parachute deployment.

The reconstructed trajectory state at parachute deployment for both vehicles is compared against an existing reconstruction found in [2]. Table 4 shows the numerical comparison between the reconstructions. The current reconstruction agrees well with the existing reconstruction.

Table 4: MER Parachute Deployment Reconstructed State Comparison Between Reference [2] and Current Reconstruction

| Parameter | Spirit( [2]) | Spirit | Opportunity( [2]) | Opportunity |
|---|---|---|---|---|
| Time - $t_{ref}$ (SCLK sec) | 2336.375 | 2336.375 | 8444.625 | 8444.625 |
| Altitude (km) | 7.5 | 7.655 | 6.2 | 7.24 |
| Relative Velocity (m/s) | 410.98 | 408.5 | 429.68 | 428.6 |
| Latitude (deg N) | -14.528 | -14.76 | -1.957 | -1.992 |
| Longitude (deg E) | 175.411 | 176.3 | 354.413 | 355.4 |

For Spirit, radar altimeter data is compared to the reconstructed trajectory as shown in Figure 10. The reconstructed trajectory agrees well with the altimeter data in terms of altitude and velocity. Shortly after the retrorocket initiation, the backshell accelerometer data abruptly zeros out. This leads to the reconstructed trajectory diverging from the altimeter data. Additionally upon the bridle being cut, the backshell-based IMU data will not provide the relevant data for the landing sequence. These errors can be potentially reconciled if rover-based transformed IMU data is available and utilized in the reconstruction.

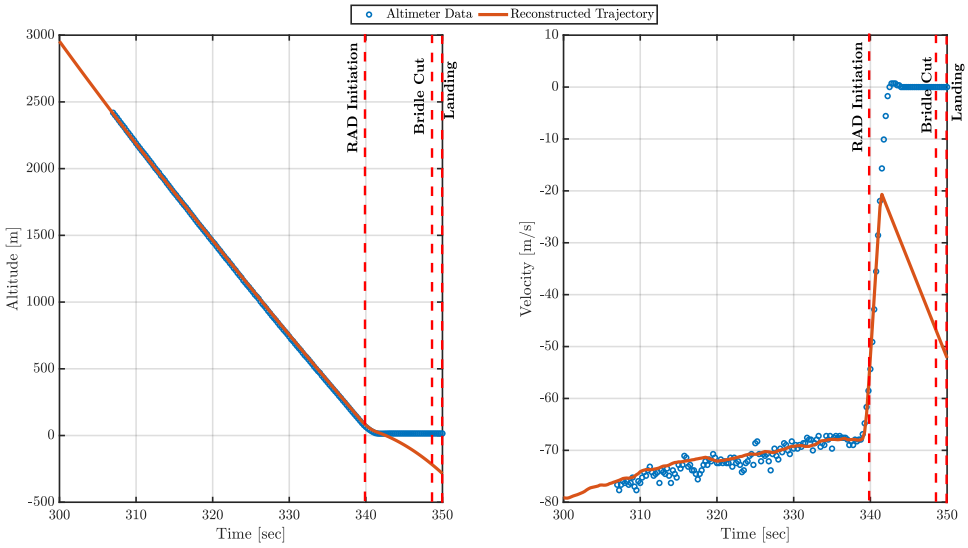


Figure 10: Spirit Trajectory Comparison to radar altimeter data

Due to the lack of Opportunity transformed IMU data after parachute deployment as well as rover-based IMU data, the current reconstruction is unable to produce an accurate reconstruction of each vehicle's final landing state. However, an

estimate of the landing location can be made with the current Spirit reconstruction dataset at RAD initiation. At this point, it assumed that the vehicle descent trajectory is purely vertical with respect to the ground. Given this assumption, the landing location latitude/longitude (at first impact after bridle cut) can be approximated from the reconstructed trajectory. Table 5 provides a comparison between the landing targets and actual landing point for Spirit/Opportunity [7] to the approximated landing location with the current trajectory reconstruction. The data shows that the current reconstruction provides a suitable approximation for the landing site of Spirit.

Table 5: MER Landing Target and Actual Location Comparison to Current Reconstruction

| Vehicle | Latitude (deg N) | Longitude (deg E) |
|---|---|---|
| Spirit (Target) [7] | -14.59 | 175.3 |
| Spirit (Actual) [7] | -14.57 | 175.5 |
| Spirit (Reconstruction) | -14.74 | 176.8 |
| Opportunity (Target) [7] | -1.98 | 354.06 |
| Opportunity (Actual) [7] | -1.95 | 354.47 |
| Opportunity (Reconstruction) | – | – |

### 5.2 Atmospheric-Relative Trajectory

This section describes the atmospheric-relative trajectory that was reconstructed from the reconstructed inertial trajectory, transformed IMU acceleration data, and the nominal aerodynamic database. Although zero degree total angle of attack is assumed to keep the vehicle attitude constant in the trajectory reconstruction process, the actual reconstructed total angle of attack may not be identically zero but close to zero.

Figure 11 depicts the reconstructed atmosphere-relative trajectory as described by each vehicle's axial force coefficient, freestream dynamic pressure, freestream Mach number, and total angle of attack. The results are presented from 70 sec after entry interface to parachute deployment. The reconstructed axial force coefficient profile for Spirit and Opportunity are nearly identical with small differences due to the reconstructed total angle of attack. Spirit reconstructed data shows higher flown total angle of attack and as a result a slightly lower axial force coefficient as compared to Opportunity. The reconstructed dynamic pressure profiles are also nearly identical with Opportunity achieving a higher peak value. Likewise, the reconstructed Mach number profiles are also similar. Despite having different values, the total angle of attack profiles between Spirit and Opportunity are similar. Between 70-100 sec, both vehicles exhibit small amplitude oscillations in total angle of attack. Additional oscillations can be seen around Mach 15 (most pronounced in reconstructed Opportunity profile) and in the supersonic regime below Mach 5.

These trend are consistent with preflight EDL trajectory analysis that indicated potential pitching moment instabilities about Mach 27, Mach 16, and portions of the supersonic flow regime at low total angles of attack [4]. At parachute deployment, the reconstructed dynamic pressure and Mach number is 766 Pa, 647.1 Pa and 1.817, 1.67 for Opportunity and Spirit respectively. These dynamic pressure values are consistent with the anticipated nominal parachute deployment pressure of 700 $N/m^2$.

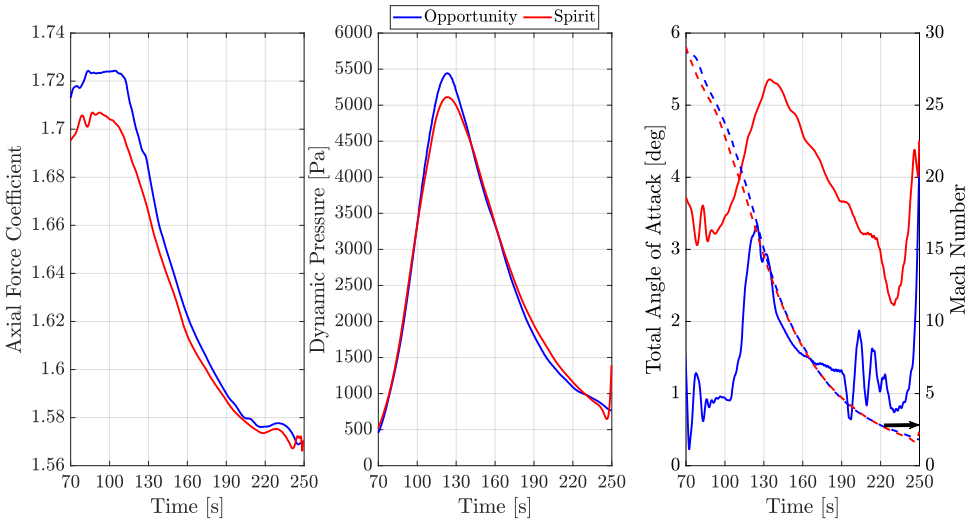


Figure 11: Atmospheric-Relative Trajectory

Finally, the time histories of the atmospheric conditions along the reconstructed trajectory are shown in Figure 12. Here, the density is reconstructed from dynamic pressure and atmospheric-relative velocity (assuming zero nominal wind profile). Pressure is computed from the reconstructed altitude and integration of the hydrostatic equation, and lastly temperature is computed from the ideal gas law. The reconstructed density profiles between each vehicle are nearly identical for low altitudes but exhibit differences at high altitudes. Similar trend can be seen for the pressure and temperature profiles as well.

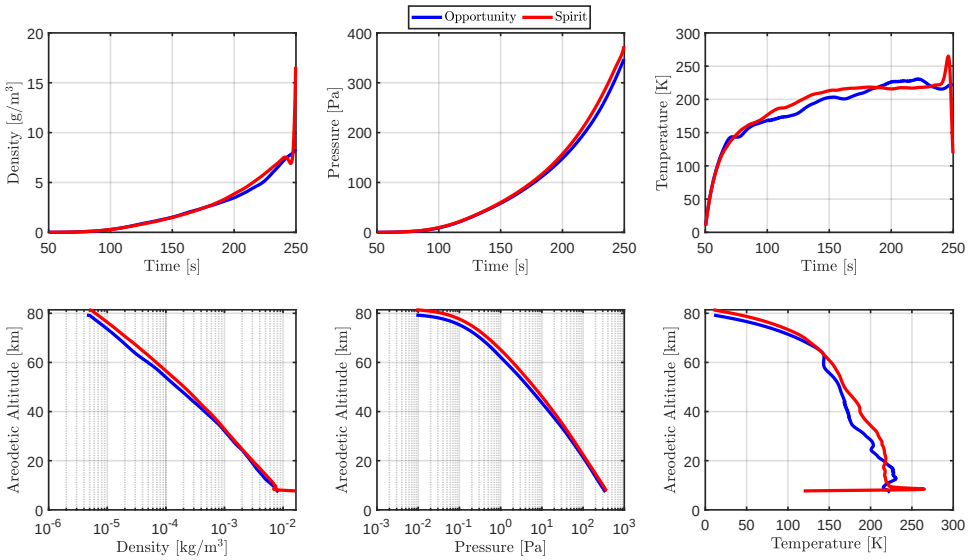


Figure 12: Atmosphere

## 5.3 Atmosphere Reconstruction

Figure 13 shows a comparison of the current reconstructed atmospheric density profiles of Spirit and Opportunity to previous ones found in Reference [2]. The current reconstruction agrees well with the previous one.

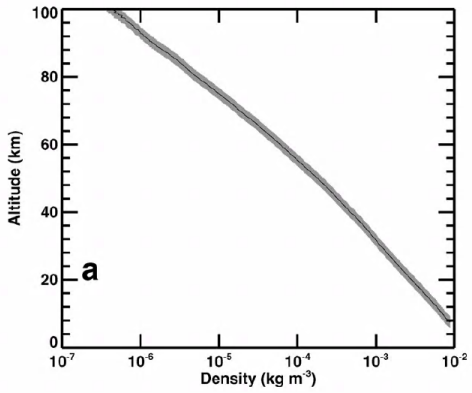


(a) Spirit (Reference [2])

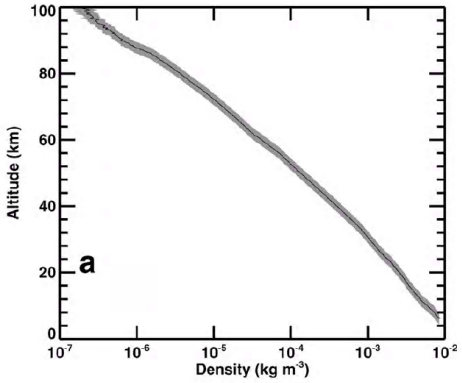


(b) Opportunity (Reference [2])

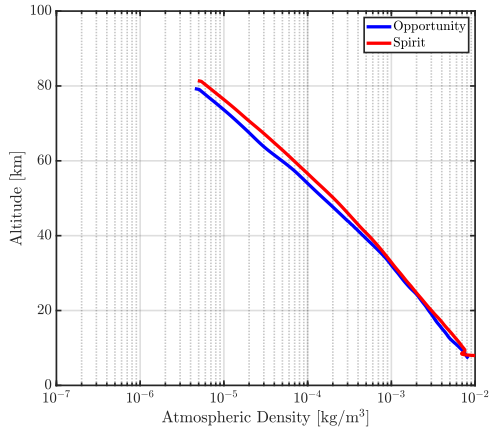


(c) Current Work

Figure 13: Comparison of Reconstructed Atmospheric Density Profiles. The greyed regions in (a) and (b) indicate the reconstructed density profile uncertainty bounds and the black solid line indicates the deterministic reconstructed profile.

# 6 Trajectory Conditions

A summary of the conditions at several events on the trajectory reconstruction for Spirit and Opportunity are provided in Table 6 and Table 7, respectively. Key events are from atmospheric entry to parachute deployment. Due to Knudsen number dependence, values for Mach, dynamic pressure, and total angle of attack were not computed using Phoenix aerodatabase in atmospheric reconstruction.

Table 6: Spirit trajectory conditions at key events

| **Event** | **Time from $t_0$** *sec* | **Mach** | **Dynamic Pressure** *Pa* | **Wind-Relative Velocity** *m/s* | **Areodetic Altitude** *km* | **Planet-Relative Flight Path Angle** *deg* | **Total Angle Of Attack** *deg* |
|---|---|---|---|---|---|---|---|
| Initialization | 0 | – | – | 5399 | 131.1 | -11.99 | – |
| Mach 25 | 90.5 | 25 | 2181 | 5107 | 51.89 | -6.773 | 3.255 |
| Mach 20 | 110.8 | 20 | 4471 | 4342 | 41.23 | -5.95 | 3.949 |
| Peak Dynamic Pressure | 123.3 | 16.51 | 5112 | 3660 | 36.15 | -5.726 | 4.857 |
| Mach 15 | 128.5 | 15 | 5038 | 3366 | 34.32 | -5.715 | 5.095 |
| Mach 10 | 149.5 | 10 | 3980 | 2324 | 28.24 | -6.246 | 4.963 |
| Mach 5 | 186.8 | 5 | 2066 | 1171 | 20.02 | -9.919 | 3.731 |
| Parachute Deployment | 246.3 | 1.67 | 647.1 | 431.3 | 8.385 | -26.82 | 4.382 |

Table 7: Opportunity trajectory conditions at key events

| **Event** | **Time from $t_0$** *sec* | **Mach** | **Dynamic Pressure** *Pa* | **Wind-Relative Velocity** *m/s* | **Areodetic Altitude** *km* | **Planet-Relative Flight Path Angle** *deg* | **Total Angle Of Attack** *deg* |
|---|---|---|---|---|---|---|---|
| Initialization | 0 | – | – | 5455 | 129.3 | -11.99 | |
| Mach 25 | 93.75 | 25 | 2509 | 5095 | 47.99 | -6.423 | 0.9371 |
| Mach 20 | 114.3 | 20 | 5042 | 4198 | 37.97 | -5.582 | 2.13 |
| Peak Dynamic Pressure | 123.3 | 17.29 | 5443 | 3662 | 34.58 | -5.418 | 3.268 |
| Mach 15 | 130 | 15 | 5197 | 3259 | 32.38 | -5.396 | 2.895 |
| Mach 10 | 150 | 10 | 3886 | 2262 | 27.09 | -5.904 | 1.743 |
| Mach 5 | 186 | 5 | 1953 | 1169 | 19.68 | -9.458 | 1.321 |
| Parachute Deployment | 249.8 | 1.817 | 766 | 249.8 | 7.24 | -27.43 | 4.1 |

# 7 Conclusions

The NewSTEP Kalman filter trajectory reconstruction code was used to reconstruct the Mars Exploration Rovers entry, descent, and landing trajectory and the day of landing atmosphere. All available data was used in the reconstruction process, including initial conditions, inertial measurement unit and radar altimeter. The trajectory and atmosphere reconstruction results compared well with published results from previous MER reconstructions.

One of the challenges faced in this reconstruction effort was the lack of available data. This limited the scope and fidelity of the reconstructed trajectories. Future work may include incorporating more flight data, if they still exist, into the reconstruction effort. Once a complete deterministic reconstructed solution is obtained, the introduction of uncertainties into the reconstruction process can be done. Utilizing NewSTEP extended Kalman filter, a probabilistic reconstruction can be obtained.

# 8 Appendix

Listed below are the data sources utilized in this paper trajectory reconstruction process. These data sources are archived in the NASA Langley EDL Cluster for future reference.

The raw IMU data sources for MER-1 (Opportunity) and MER-2 (Spirit) can be found in "1HIGHRATE.tab" and "2HIGHRATE.tab". The corresponding transformed IMU data can be found "1TRANSFORMED.tab" and "2TRANSFORMED.tab". The provided data is converted to *MATLAB* tables. For Spirit, EDL telemetry data provides the dynamic buffer contents for the transformed IMU data as well as radar altimeter data. These corresponding files are titled "dyndata.txt" and "rasdata.txt".

# References


1. Blanchard, R. C., "Entry Descent and Landing Trajectory and Atmosphere Reconstruction for the Mars Exploration Rovers Missions A and B," Technical Report, The George Washington University, Grant Award No. CCLS20568F, April 2008.

2. Withers, P. and Smith, M. D., "Atmospheric entry profiles from the Mars Exploration Rovers Spirit and Opportunity," *Icarus*, Vol. 185, No. 1, 2006, pp. 133–142.

3. Desai, P. N. and Knocke, P. C., "Mars Exploration Rovers Entry, Descent, and Landing Trajectory Analysis," *Journal of Astronautical Sciences*, Vol. 55, No. 1, 2007, pp. 311–323.

4. Desai, P. N. and Schoenenberger, M. and Cheatwood, F. M, "Mars Exploration Rover Six-Degree-of-Freedom Entry Trajectory Analysis," *Journal of Spacecraft and Rockets*, Vol. 43, No. 5, 2006, pp. 1019–1025.

5. Karlgaard, C. D. and Tynis, J. A., "Mars Phoenix EDL Trajectory and Atmosphere Reconstruction Using NewSTEP," NASA TM-2019-220282.

6. Schoenenberger, M. and Cheatwood, F. M. and Desai, P. N., "Static Aerodynamics of the Mars Exploration Rover Entry Capsule," AIAA Paper 2005–56, January 2005.

7. Knocke, P. C. and Wawrzyniak, G. G. and Kennedy, B. M. and Desai, P. N. and Parker, T. J. and Golombek, M., P. and Duxbury, T. C. and Kass, D. M., "Mars Exploration Rovers Landing Dispersion Analysis," AIAA Paper 2004–5093, August 2004.

8. Crisp, J. A., and Adler, M., and Matijevic, J. R., and Squyres, S. W., and Arvidson, R. E., and Kass, D. M., "Mars Exploration Rover mission" *Journal of Geophysical Research*, Vol. 108, No. 8061, 2003.

9. Korzun, A. M. and Maddock, R. W. and Schoenenberger, M., and Edquist, K. T. and Zumwalt, C. H. and Karlgaard, C. D. "Aerodynamic Performance of the 2018 InSight Mars Lander," AIAA Paper 2020–1272, January 2020.

10. Crassidis, J. L., and Junkins, J. L., *Optimal Estimation of Dynamic Systems*, CRC Press, Boca Raton, FL, 2004, Chapter 5.

11. Portock, B. M., Kruizinga, G., Bonfiglio, E., Raofi, B., and Ryne, M., "Navigation Challenges of the Mars Phoenix Lander Mission," AIAA Paper 2008–7214, August 2008.

12. Tapley, B. D., Schutz, , B. E., and Born, G. H., *Statistical Orbit Determination*, Elsevier, 2004, Chapter 2.

13. Karlgaard C. D., Tartabini, P. V., Blanchard, R. C., Kirsch, M., and Toniolo, M. D., "Hyper-X Post-Flight-Trajectory Reconstruction," *Journal of Spacecraft and Rockets*, Vol. 43, No. 1, 2006, pp. 105–115.

14. Karlgaard, C. D., Beck, R. E., Derry, S. D., Brandon, J. M., Starr, B. R., Tartabini, P. V., and Olds, A. D., "Ares I-X Trajectory Reconstruction: Methodology and Results," *Journal of Spacecraft and Rockets*, Vol. 50, No. 3, 2013, pp. 641–661.

15. Karlgaard, C. D., Kutty, P., Schoenenberger, M., Munk, M. M., Little, A., Kuhl, C. A., and Shidner, J., "Mars Science Laboratory Entry Atmospheric Data System Trajectory and Atmosphere Reconstruction," *Journal of Spacecraft and Rockets*, Vol. 51, No. 4, 2014, pp. 1029–1047.

16. Karlgaard, C. D., Kutty, P., O'Farrell, C., Blood, E., Ginn, J., and Schoenenberger, M., "Reconstruction of Atmosphere, Trajectory, and Aerodynamics for the Low-Density Supersonic Decelerator Project," *Journal of Spacecraft and Rockets*, Vol. 56, No. 1, 2019, pp. 221–240.

17. Karlgaard, C. D., Korzun, A. M., Schoenenberger, M., Bonfiglio, E. P., Kass, D. M., Grover, M. R., "Mars InSight Entry, Descent, and Landing Trajectory and Atmospheric Reconstruction," AIAA Paper 2020–1271, January 2020.

18. Kutty, P. and Karlgaard, C. D., "Mars Science Laboratory Aerodatabase Trajectory Reconstruction and Uncertainty Assessment," AIAA Paper 2014-1094, January 2014.

19. Kutty, P., "Reconstruction and Uncertainty Quantification of Entry, Descent, and Landing Trajectories Using Vehicle Aerodynamics," M. S. Thesis, School of Aerospace Engineering, Georgia Institute of Technology, May 2014.

20. Edquist, K. T., Desai, P. N., and Schoenenberger, M., "Aerodynamics for Mars Phoenix Entry Capsule," *Journal of Spacecraft and Rockets*, Vol. 48, No. 5, 2011, pp. 713–726.

21. Konopliv, A. S., Asmar, S. W., Folkner, W. M., Karatekin, O., Nunes, D. C., Smrekar, S. E., Yoder, C. F., and Zuber, M. T., "Mars High Resolution Gravity Fields from MRO, Mars Seasonal Gravity, and Other Dynamical Parameters," *Icarus*, Vol. 211, No. 1, 2011, pp. 401–428.

| REPORT DOCUMENTATION PAGE | Form Approved OMB No. 0704–0188 |
|---|---|



| 1. REPORT DATE *(DD-MM-YYYY)* | 2. REPORT TYPE | 3. DATES COVERED *(From - To)* |
|---|---|---|
| 01-05-2021 | Technical Memorandum | |

**4. TITLE AND SUBTITLE**
Mars Exploration Rovers EDL Trajectory and Atmosphere Reconstruction Using NewSTEP

**5a. CONTRACT NUMBER**

**5b. GRANT NUMBER**

**5c. PROGRAM ELEMENT NUMBER**

**6. AUTHOR(S)**
Rohan G. Deshmukh and Christopher D. Karlgaard

**5d. PROJECT NUMBER**

**5e. TASK NUMBER**

**5f. WORK UNIT NUMBER**
80LARC17C0003

**7. PERFORMING ORGANIZATION NAME(S) AND ADDRESS(ES)**
NASA Langley Research Center
Hampton, Virginia 23681-2199

**8. PERFORMING ORGANIZATION REPORT NUMBER**

**9. SPONSORING/MONITORING AGENCY NAME(S) AND ADDRESS(ES)**
National Aeronautics and Space Administration
Washington, DC 20546-0001

**10. SPONSOR/MONITOR'S ACRONYM(S)**
NASA

**11. SPONSOR/MONITOR'S REPORT NUMBER(S)**
NASA/TM–20210015330

**12. DISTRIBUTION/AVAILABILITY STATEMENT**
Unclassified-Unlimited
Subject Category 64
Availability: NASA STI Program (757) 864-9658

**13. SUPPLEMENTARY NOTES**
An electronic version can be found at http://ntrs.nasa.gov.

**14. ABSTRACT**

This document describes the trajectory and atmosphere reconstruction of the Mars Exploration Rovers (Spirit and Opportunity) Entry, Descent, and Landing using the New Statistical Trajectory Estimation Program. The approach utilizes a Kalman filter to blend inertial measurement unit data with initial conditions and radar altimetry to obtain the inertial trajectory of the entry vehicle. The nominal aerodynamic database is then used in combination with the sensed accelerations to obtain estimates of the atmosphere-relative state. The reconstructed atmosphere profile is then blended with pre-flight models to construct an estimate of the as-flown atmosphere.

**15. SUBJECT TERMS**
Mars Exploration Rovers, Trajectory Reconstruction, EDL, Kalman Filtering, Inertial Navigation

| 16. SECURITY CLASSIFICATION OF: | | | 17. LIMITATION OF ABSTRACT | 18. NUMBER OF PAGES | 19a. NAME OF RESPONSIBLE PERSON |
|---|---|---|---|---|---|
| a. REPORT | b. ABSTRACT | c. THIS PAGE | | | STI Information Desk (help@sti.nasa.gov) |
| U | U | U | UU | 27 | 19b. TELEPHONE NUMBER *(Include area code)* (757) 864-9658 |